Pediatr Radiol (2010) 40:999–1009
DOI 10.1007/s00247-010-1613-y

REVIEW

New MR sequences (diffusion, perfusion, spectroscopy) in brain tumours

Andrea Rossi · Carlo Gandolfo · Giovanni Morana · Mariasavina Severino · Maria Luisa Garrè · Armando Cama

Received: 15 January 2010 / Accepted: 24 January 2010

Abstract While MRI has been instrumental in significantly improving care in children harbouring brain tumours, conventional sequences lack information regarding functional parameters including cellularity, haemodynamics and metabolism. Advanced MR imaging modalities, such as diffusion (including diffusion tensor imaging and fibre tractography), perfusion and spectroscopy have significantly improved our understanding of the physiopathology of brain tumours and have provided invaluable additional information for treatment planning and monitoring of treatment results. The contribution of these methods to the characterization of brain neoplasms in children is the focus of the present manuscript.

Keywords Brain · MR · Diffusion · Perfusion · Spectroscopy · Child

Introduction

Brain tumours are the second most common group of childhood malignancies after leukaemia. Contrary to adults, most childhood brain tumours are primitive lesions. The most common location is the posterior cranial fossa, where tumours predominate between 1 and 11 years of age. Conversely, tumours occurring in children younger than 1 year and older than 12 years are more commonly located in the supratentorial compartment. MRI has provided an invaluable tool in the identification and characterization of childhood brain tumours as well as in the presurgical planning and evaluation of treatment results, including the outcomes of surgery, chemotherapy and irradiation. However, conventional MRI provides little, if any, information regarding functional features including tumour cellularity, haemodynamics and metabolism. These shortcomings have been largely overcome by the introduction of advanced MR imaging modalities, including diffusion, perfusion, and spectroscopy [1]. The contribution of these methods to the characterization of brain neoplasms is the focus of the present manuscript.

A. Rossi (✉) · C. Gandolfo · G. Morana · M. Severino
Pediatric Neuroradiology, G. Gaslini Children's Research Hospital,
Largo G. Gaslini 5,
Genova 16147, Italy
e-mail: andrearossi@ospedale-gaslini.ge.it

M. L. Garrè
Pediatric Neuro-oncology, G. Gaslini Children's Research Hospital,
Largo G. Gaslini 5,
Genova 16147, Italy

A. Cama
Pediatric Neurosurgery, G. Gaslini Children's Research Hospital,
Largo G. Gaslini 5,
Genova 16147, Italy

MR diffusion

Diffusion-weighted imaging (DWI) provides information regarding diffusion of water molecules in the section studied, from which quantitative values, the so-called apparent diffusion coefficient (ADC), can be calculated. In the normal brain, diffusion of water depends on several factors, the most important being the orientation of axon and myelin sheaths in the white matter tracts. In these regions, diffusion is anisotropic, i.e. it occurs efficiently along the orientation of the tracts but is restricted in orthogonal planes. This information is translated into diffusion tensor imaging (DTI) and fibre tractography that is a three-dimensional representation of MR diffusion that allows evaluation of the white matter structure and architecture.

DWI is useful to differentiate between ring-enhancing lesions that can represent either bacterial abscess or necrotic tumour on conventional MRI; restricted diffusion within the necrotic cavity indicates an abscess, whereas tumour

necrosis has increased diffusion [2]. Another traditional application of DWI is the differentiation of epidermoids from arachnoid cysts, in which the former produces restricted diffusion and the latter increased, water-like diffusion [3]. However, the most important application of DWI in the field of brain tumour imaging is the estimation of cellularity that is a function of tumour grading. In general, ADC values are inversely correlated with tumour grade, i.e. low-grade tumours (Fig. 1) have higher ADCs than high-grade tumours (Fig. 2), although some degree of overlap exists between certain tumour types [4]. This information may be crucial when histological verification is lacking or hazardous, as is the case with some brainstem tumours. An important caveat is that ADC values should be evaluated in the solid tumour portions, without including calcified, haemorrhagic or necrotic areas. ADC values can be significantly higher within necrotic portions of high-grade tumours and may lead to an inaccurate estimate of cellularity.

DTI and fibre tractography are important tools for preoperative mapping of brain tumours including the identification of relationships to functional areas such as major fibre tracts (Fig. 3). The graphic representation of the latter is co-registered on 3-D anatomic MR images that can be visualized in multiple planes and transferred to the neuronavigator in the surgical room, thereby allowing for preservation of intact brain while maximizing the extent of surgical resection. DTI identifies four main patterns of the

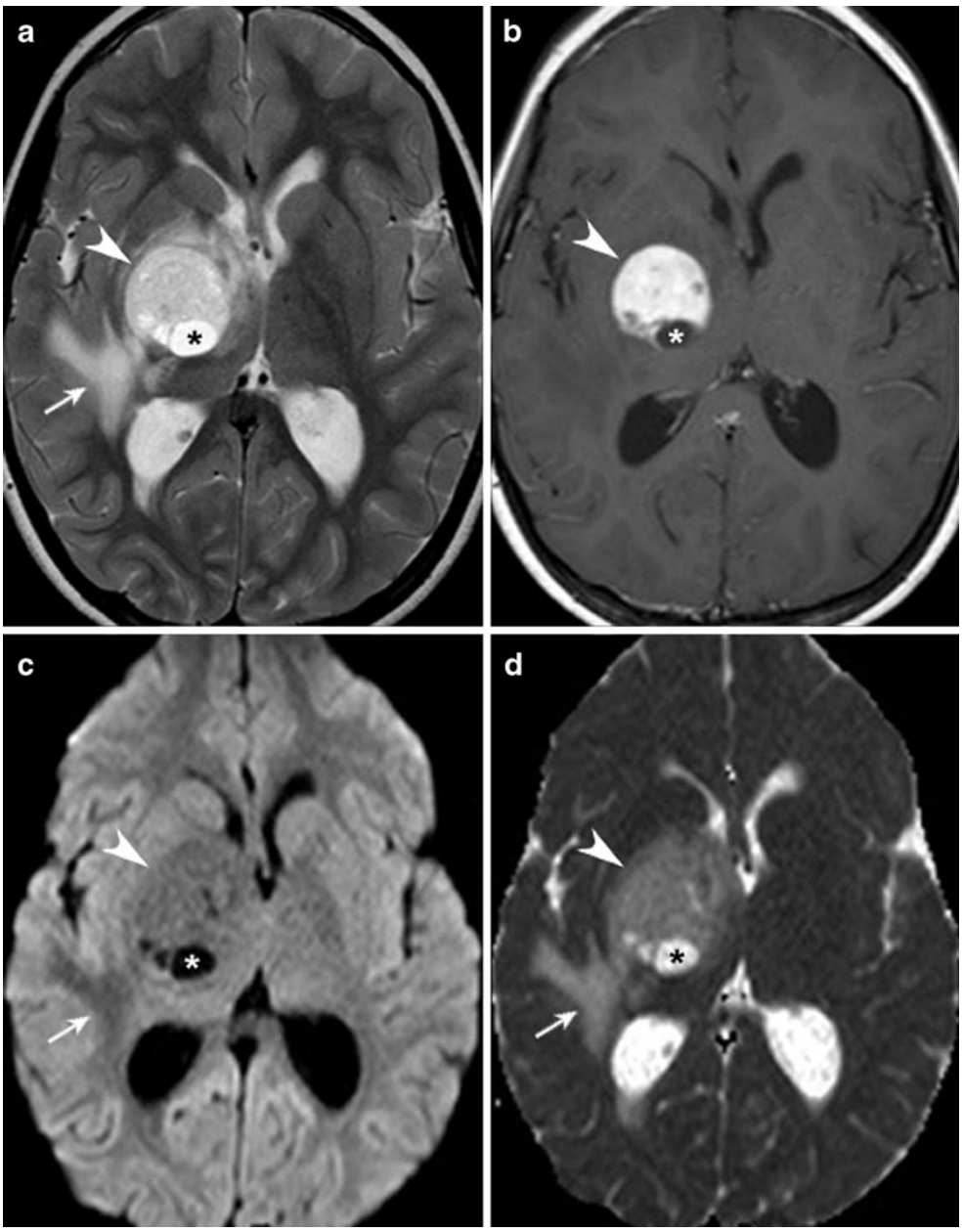

Fig. 1 MRI of a pilocytic astrocytoma (grade I) of the right nucleocapsular region in a 5-year-old girl. Axial T2-weighted image (**a**), contrast-enhanced axial T1-weighted image (**b**), axial diffusion-weighted image (**c**) and corresponding ADC map (**d**). The solid portion of the lesion (*arrowheads*) is T2 hyperintense, enhances markedly and has increased diffusion as shown by hyperintensity on the ADC map. There is a small cystic component (*asterisk*). Note concurrent vasogenic oedema (*arrow*)

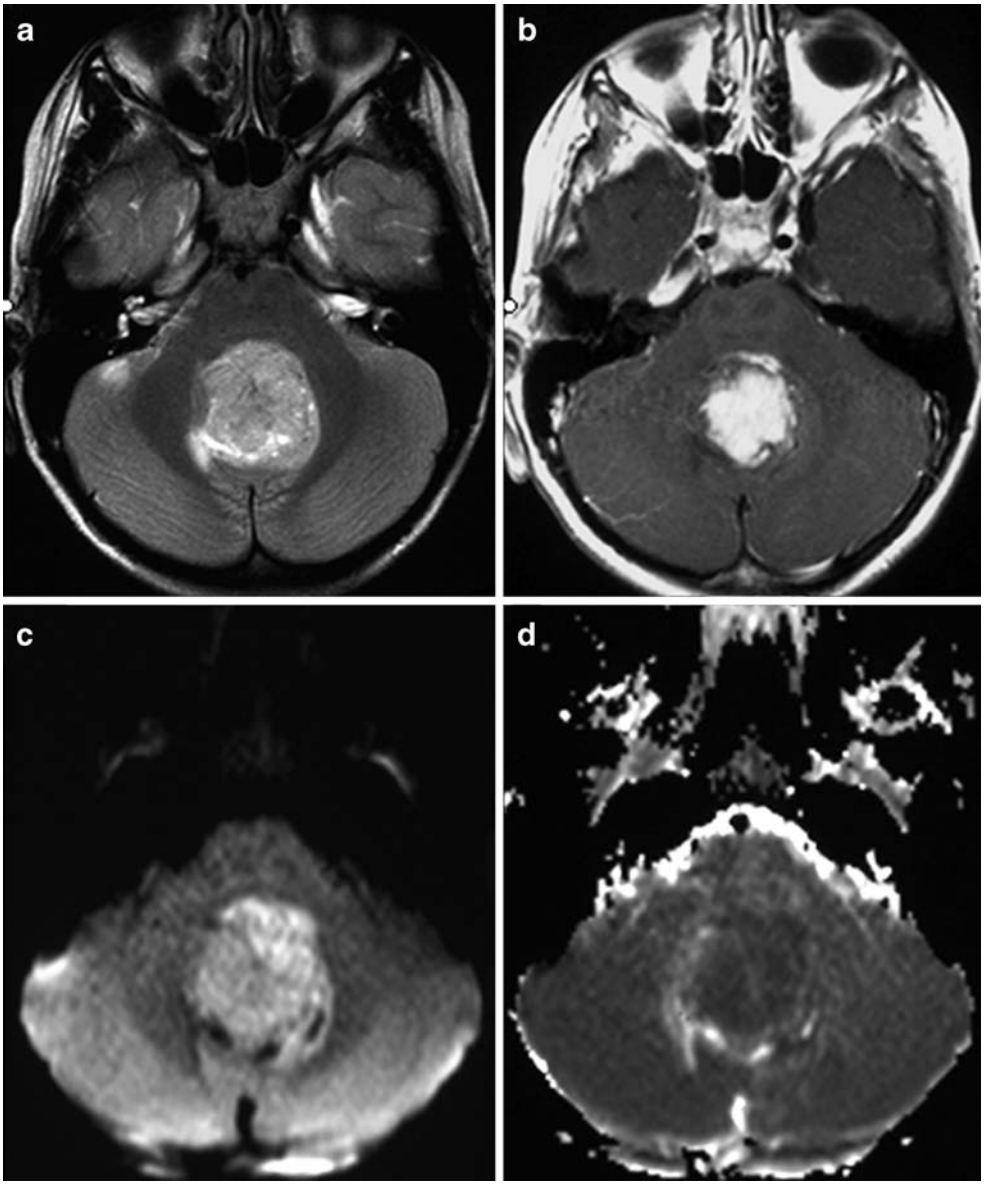

Fig. 2 MRI of a medulloblastoma (grade IV) in a 4-year-old boy. Axial T2-W image (**a**), contrast-enhanced axial T1-W image (**b**), axial diffusion-weighted image (**c**) and corresponding ADC map (**d**). This solid tumour is T2 isointense to gray matter and enhances inhomogeneously. The lesion has uniformly restricted diffusion consistent with its hypercellular nature

relationship between tumour and fibre tracts, i.e. deviation, oedema, infiltration and destruction [5]. Applications of DTI are obviously greater in supratentorial lesions that are located in the deep regions of the hemispheres such as the nucleocapsular regions, corona radiata, centrum ovale or corpus callosum. The additional scan time for inclusion of DTI in the scan protocol is between 5 min and 10 min on most clinical high-field scanners, mainly depending on the selected number of encoding directions as well as the use of parallel imaging techniques.

MR perfusion

Perfusion-weighted imaging (PWI) measures cerebral haemodynamics at the microcirculation level. Several parameters can be measured by PWI, including cerebral blood volume (CBV), cerebral blood flow (CBF) and mean transit time (MTT). Of these, the CBV, defined as the volume of blood in an area of brain tissue expressed in ml/100 g, is the most commonly evaluated in the field of brain tumour imaging [6]. There are several techniques for performing PWI. The most widely available is T2*-weighted dynamic susceptibility contrast (DSC) imaging. This requires the bolus intravenous administration of a paramagnetic contrast medium and the rapid acquisition of images over time during the first pass of contrast material through the capillary bed [7]. This is typically obtained by means of echo-planar imaging. DSC-PWI poses a number of technical challenges in children [8]. These include the need for constant, high-flow contrast medium injection, requiring the use of power injectors and stable, sufficiently sized intravenous access catheters that may be difficult to apply safely especially in the newborn and infant age groups.

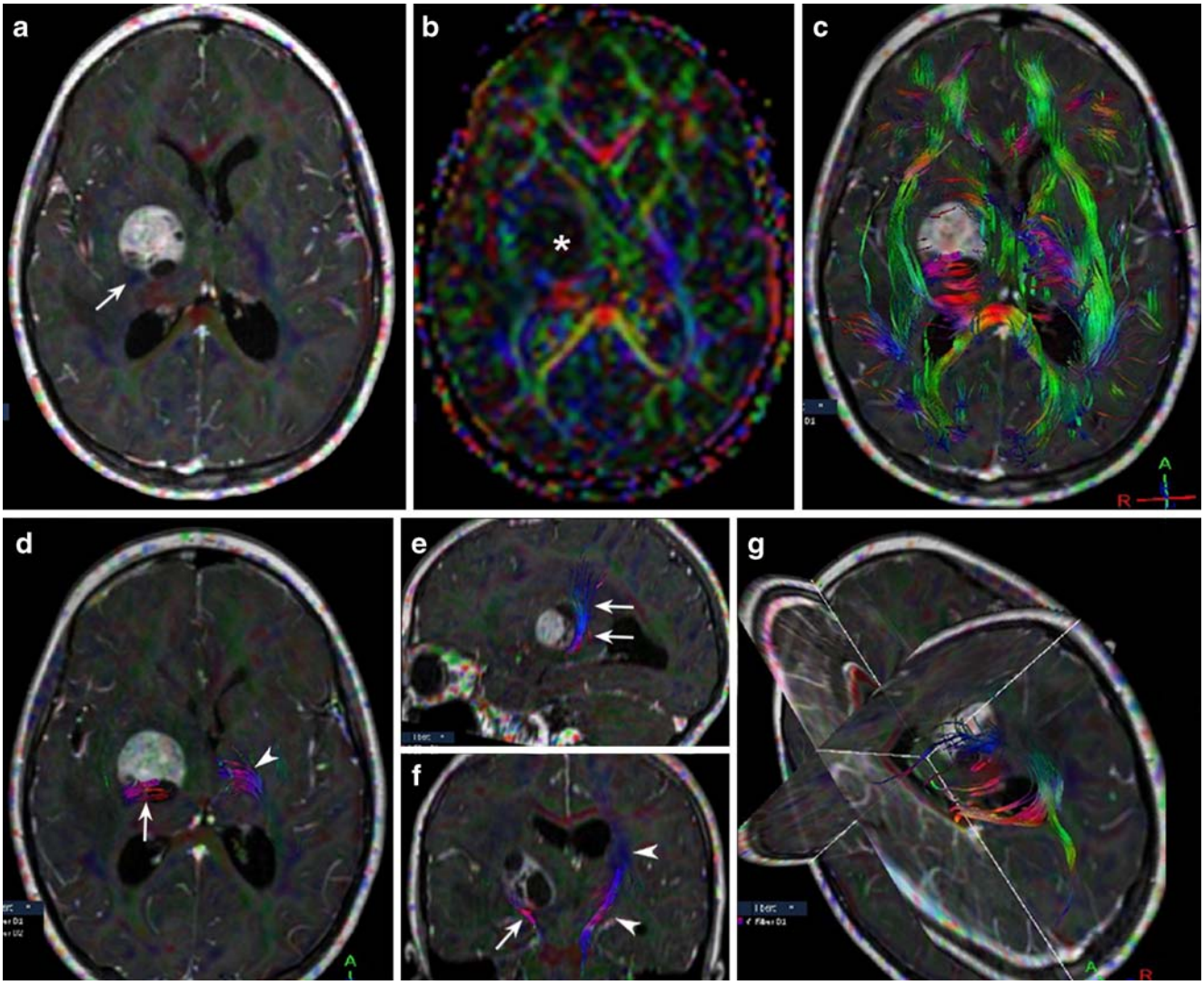

Fig. 3 DTI in a 5-year-old girl with pilocytic astrocytoma (grade I). Coregistered contrast-enhanced axial T1-W image (**a**) and fractional anisotropy (FA) map (**b**) show location of the tumour in the right nucleocapsular region with involvement of the posterior limb of the internal capsule. The pyramidal tract shows up as a blue dot (*arrow*) just posterior to the mass. The colour-coded FA map shows that the tumour has isotropic diffusion (*asterisk*). Fibre tractography (**c**) shows orientation of the various fibre tracts with respect to the enhancing mass. Fibre tractography (**d–f**) with selective tracking of the pyramidal tracts shows relationships of the mass to the right pyramidal tract that is displaced posteriorly (*arrows*). Note normal course of the left pyramidal tract (*arrowheads*). Multiplanar reformatting (g) is remotely transferred to the neuronavigator

Contrast medium is typically injected as a double dose for PWI, introducing a further limitation in small children and also creating a peculiar pitfall of diffuse injection of small leptomeningeal vessels that may create a false impression of diffuse tumour spread on subsequent conventional imaging evaluation (Fig. 4). Finally, the assumption at the base of PWI interpretation is that the contrast medium remains confined to the intravascular compartment, i.e. the blood-brain barrier is intact, which obviously is not the case with the vast majority of brain tumours. Pre-imaging infusion of a small loading dose of MR contrast medium (0.05 mmol/kg) should be performed in order to preload tissues in an attempt to decrease the likelihood of large degrees of T1-enhancement and increase the accuracy of perfusion measurements (Fig. 4) [9]. Other PWI techniques, including dynamic T1-weighted contrast imaging (providing assessment of tumour permeability) and arterial spin labelling (a perfusion technique that does not use an intravenous tracer), while promising, are less widely available in the clinical arena, and their use is presently limited to few centres where high-field (3 T and higher) are available [10].

The principal application of PWI to childhood brain tumour imaging is in the field of preoperative tumour grading. As such, it can be viewed as a complementary tool to DWI (see above). The average rCBV of high-grade lesions is significantly higher (Fig. 5) than that of low-grade neoplasms

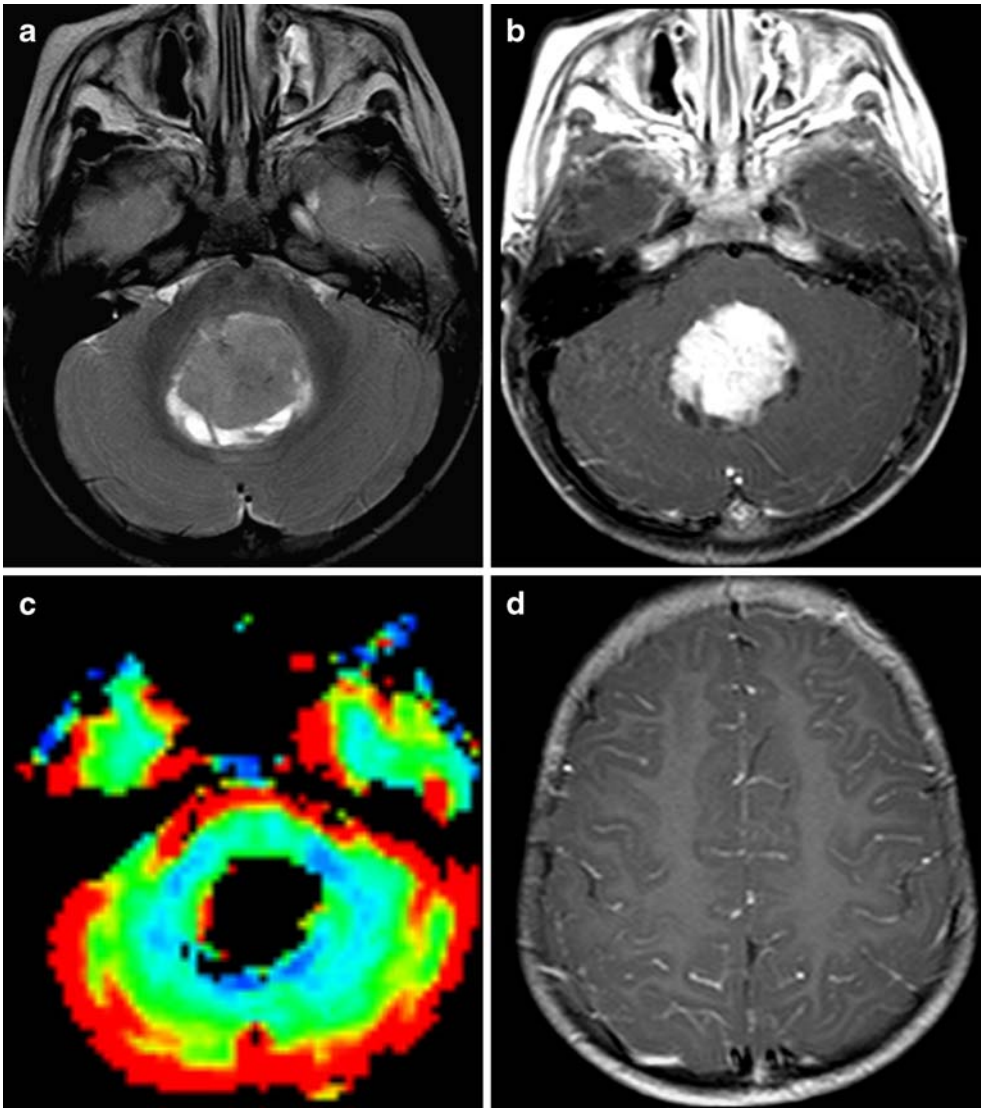

Fig. 4 Pitfalls in PWI in a 2-year-old boy with medulloblastoma (grade IV). Axial T2-W image (**a**), contrast-enhanced axial T1-W image (**b**), axial rCBV (DSC-T2*-W PWI) (**c**) and contrast-enhanced axial T1-W image (**d**). There is a T2-hypointense posterior fossa tumour (**a**) that enhances markedly with contrast medium administration (**b**) consistent with blood-brain barrier disruption. The PWI study was performed without preimaging contrast infusion, resulting in a paradoxical nulling of the rCBV (**c**). Furthermore, the double contrast material dose used for PWI resulted in a diffuse injection of subarachnoid veins, mimicking leptomeningeal tumour spread (**d**)

(Fig. 6) as a direct function of neovascularity, regardless of the degree of integrity of the blood-brain barrier [11]. Significantly, such information cannot be obtained from conventional contrast-enhanced MRI, in which the presence and degree of contrast enhancement is not only correlated to vascular hyperplasia but also to the status of the blood-brain barrier that can be altered either by destruction of normal capillaries or because of the abnormal structure of neoformed vessels; this results in the known fact that, while low-grade tumours (i.e. pilocytic astrocytomas) enhance avidly, high-grade tumours (i.e. medulloblastomas) often do not [1, 12]. Furthermore, PWI has the potential to identify progressive disease that is characterized by increase of rCBV values, as opposed to stable lesions in which rCBV does not change significantly over time [13]. Another important use of PWI is to direct stereotactic biopsy of large masses to the areas of likely higher grade that can be identified as areas of higher intralesional rCBV [14]. This application is of great significance when one considers that, other than the intrinsic morbidity, sampling errors are among the most important setbacks of brain biopsy. Finally, PWI plays an important role in the differentiation of focal radiation necrosis from residual/recurrent tumour [15]. Radiation necrosis may simulate tumour on conventional MRI, including the appearance of enhancing masses with surrounding vasogenic oedema. However, the rCBV of radiation necrosis is low due to a combination of ischaemia and vascular injury with hypoperfusion, whereas recurrent tumour is typically associated with an increase in CBV. However, the application of PWI to this peculiar area is rare in children, since focal radiation necrosis has become an exceptional finding under the current radiotherapy protocols.

MR spectroscopy

MR spectroscopy (MRS) allows noninvasive detection and measurement of normal and abnormal metabolites and

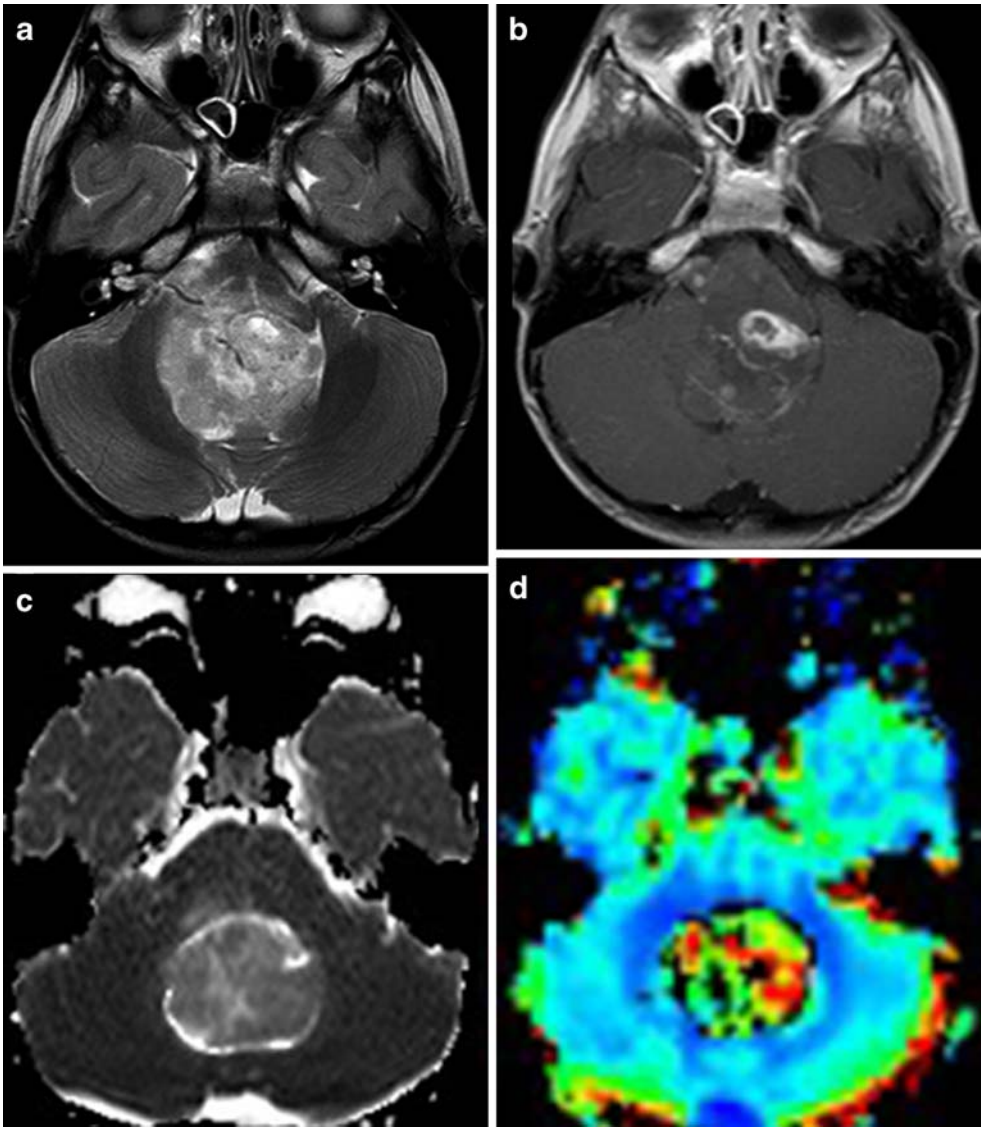

Fig. 5 PWI in a 5-year-old girl with anaplastic ependymoma (grade III) of the posterior cranial fossa. Axial T2-W image (**a**), contrast-enhanced axial T1-W image (**b**), axial ADC map (**c**) and axial rCBV (DSC-T2*-W PWI) (**d**).There is a tumour in the fourth ventricle that is T2 isointense signal to gray matter (**a**) and is mostly nonenhancing except for scattered nodular enhancing regions (**b**). There is restricted diffusion (**c**) and elevated rCBV (**d**) consistent with a high-grade lesion

plays an important role in the diagnostic work-up of brain tumours in children. Technically, MRS is based on the differences in resonance frequencies of normal and abnormal molecules within the nervous tissue. This allows the identification of individual metabolites that are represented graphically in the spectrum in the form of deviations from the baseline, the so-called peaks. Proton (^{1}H) MRS is presently available on clinical MRI units and can be performed automatically in most situations. Because of the narrow chemical shift range, however, only few metabolites are detectable. Available ^{1}H MRS techniques include single-voxel and multi-voxel [chemical shift imaging (CSI)] methods. Single-voxel ^{1}H MRS is more widespread and used routinely; it produces spectra from manually selected volumes of interest. Acquisition is possible at short (20–30 ms), intermediate (135–144 ms), and long (270–280 ms) echo times providing different possibilities for metabolite identification and peak analysis.

The metabolites normally detected in the brain, regardless of the adopted echo time include N-acetylaspartate (NAA), a neuronal marker; choline (Cho), a membrane marker; and creatine (Cr), an energy metabolism marker. Short echo-time techniques allow for additional metabolite identification, including myoinositol (mI), a glial marker. Other metabolites, including lactate (a marker of anaerobic glycolysis in hypoxic regions), lipids and glutamine-glutamate complexes, are undetectable in normal conditions. Thus, their identification indicates the presence of an abnormal process, although specificity is limited to a few disorders. Albeit technically possible, absolute quantification of normal or abnormal metabolites is not routinely performed. Relative changes of concentrations in the form of metabolite ratios are frequently used instead.

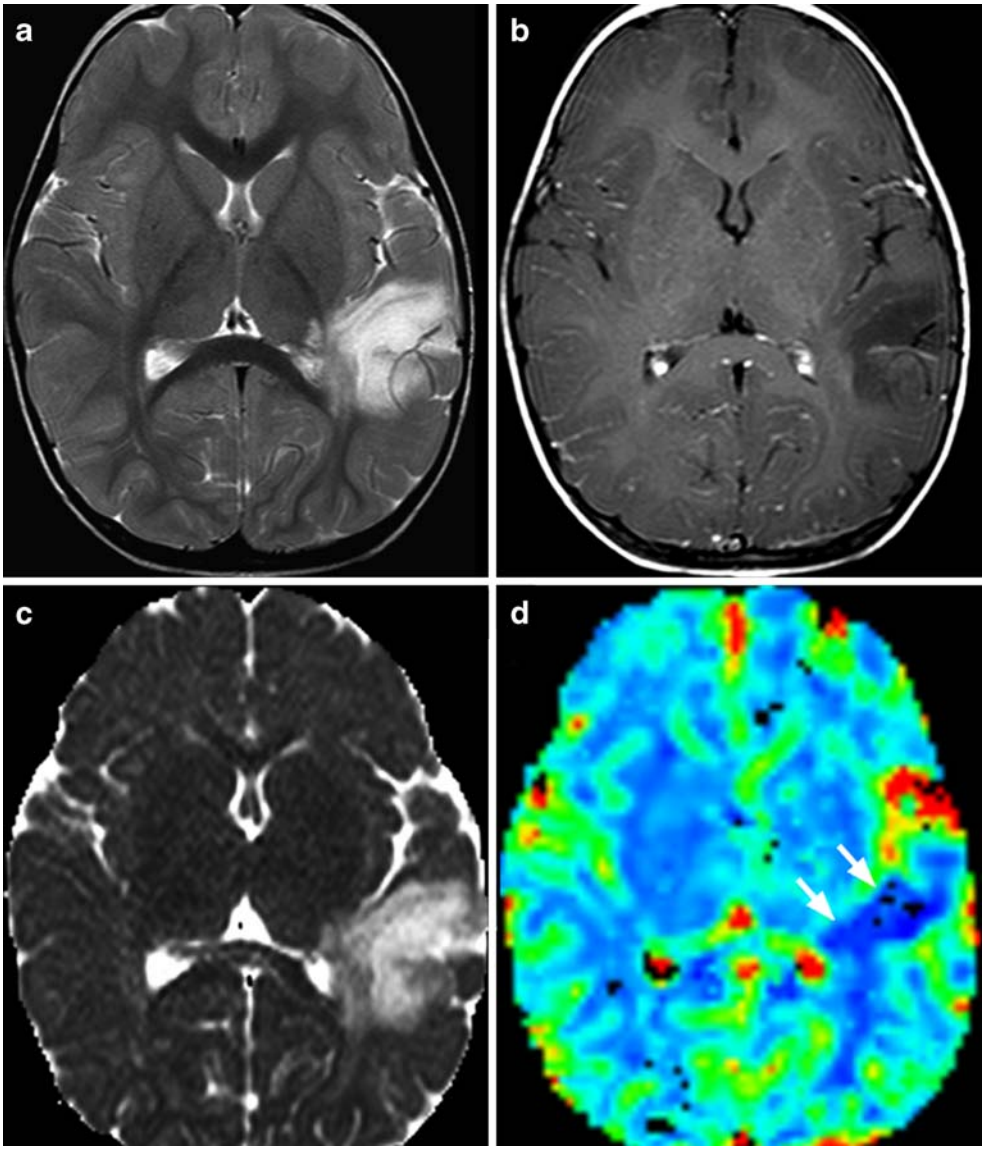

Fig. 6 PWI in a 1-year-old boy with a dysembryoplastic neuroepithelial tumor (grade I). Axial T2-W image (**a**), contrast-enhanced axial T1-W image (**b**), axial ADC map (**c**) and axial rCBV (DSC-T2*-W PWI) (**d**). There is a large cortical-subcortical lesion in the left temporo-parietal region that is T2 hyperintense (**a**) and does not enhance (**b**). The lesion shows increased diffusion with high ADC values (**a**). PWI displays low tumour rCBV (*arrows*) consistent with a low-grade neoplasm

In most instances of brain tumours, a nonspecific pathological spectrum consisting of increased Cho/Cr and decreased NAA/Cr ratios is detected, indicating loss of neuroaxonal integrity and increased myelin turnover, sometimes associated with presence of lactate, indicating impaired energy metabolism [16]. It is noteworthy that Cr, usually considered a stable peak and therefore used as an internal standard, can be markedly reduced in brain tumours because of energy impairment; thus, an increased Cho/Cr ratio can be due to elevated Cho, reduced Cr, or a combination of both [16].

Evaluation of grading has been attempted on MRS. In general, high-grade tumours have higher Cho/Cr and lower NAA/Cr ratios than low-grade ones (Fig. 7). Lipid resonances, indicative of necrosis, are frequently found in rapidly proliferating, malignant tumours including primitive neuro-ectodermal tumours (PNET), medulloblastomas (Fig. 8), and teratoid-rhabdoid tumours [17]. Lactate is typically associated with high-grade gliomas in the adult age group. However, it is important to note that lactate is frequently elevated in pilocytic astrocytomas (Fig. 7), yielding a paradoxically malignant MR spectrum for this low-grade tumour in childhood [18]. In a few instances, peculiar resonances are found that may help restrict the differential diagnosis. Of note, the presence of alanine in meningiomas yielding a inverted doublet at 1.44 parts per million (ppm) that should not be mistaken for lactate, and taurine (peak at 3.3–3.4 ppm) in PNET [19, 20]. Other important applications of MRS to the imaging of brain tumours in children include the evaluation of the peritumoural tissue for signs of invasion and the assessment of response to treatment [1]. Multi-voxel MRS can be used to identify higher grade regions within large, heterogeneous neoplasms (Fig. 9). This can be useful for directing biopsy.

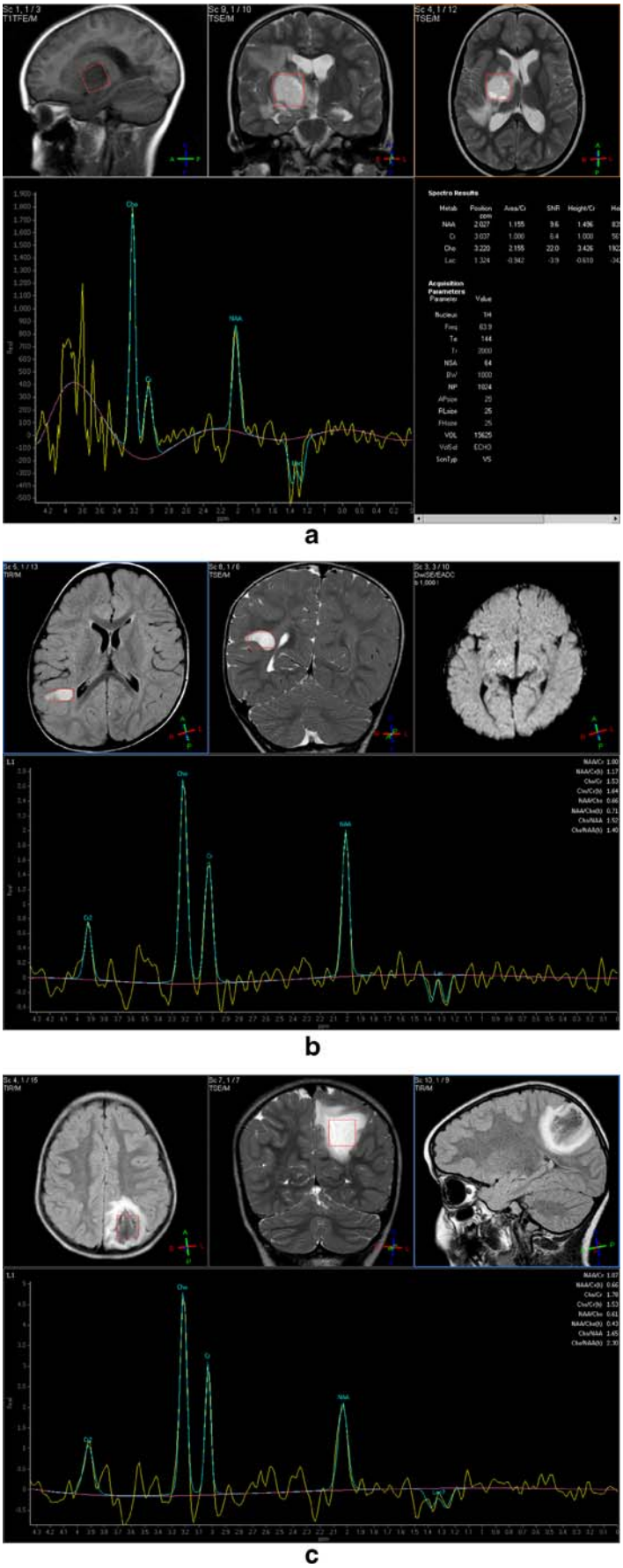

Fig. 7 Proton MRS (PRESS, TE 144 ms) in childhood gliomas. **a** Pilocytic astrocytoma (grade I) of the right nucleocapsular region in an 8-year-old girl. There is marked elevation of Cho/Cr, reduction of NAA/Cr and a readily recognizable lactate peak; the latter is a hallmark of pilocytic astrocytomas and does not indicate higher grade. **b** Diffuse astrocytoma (grade II) of the right parietal lobe in a 2-year-old boy. There is mild elevation of Cho/Cr, mild reduction of NAA/Cr, and a small lactate doublet. **c** Anaplastic astrocytoma (grade III) of the left parietal lobe in a 6-year-old girl. Increase of Cho/Cr and reduction of NAA/Cr are more prominent (compare with **b**)

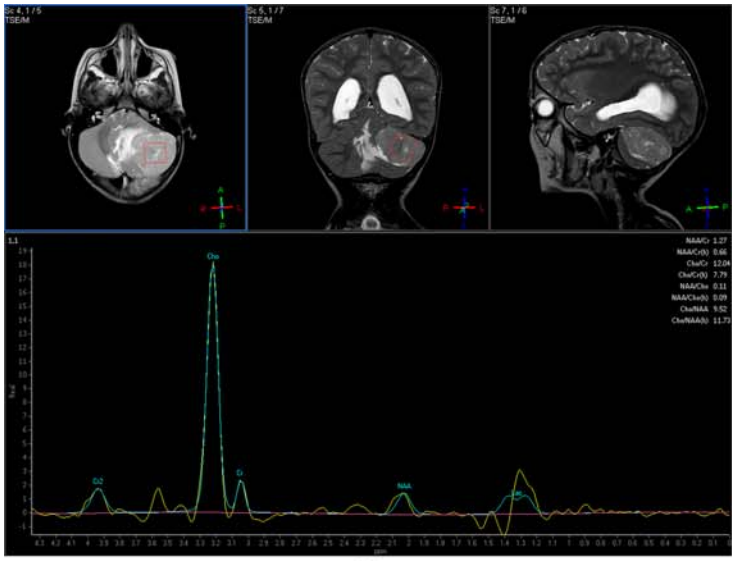

a

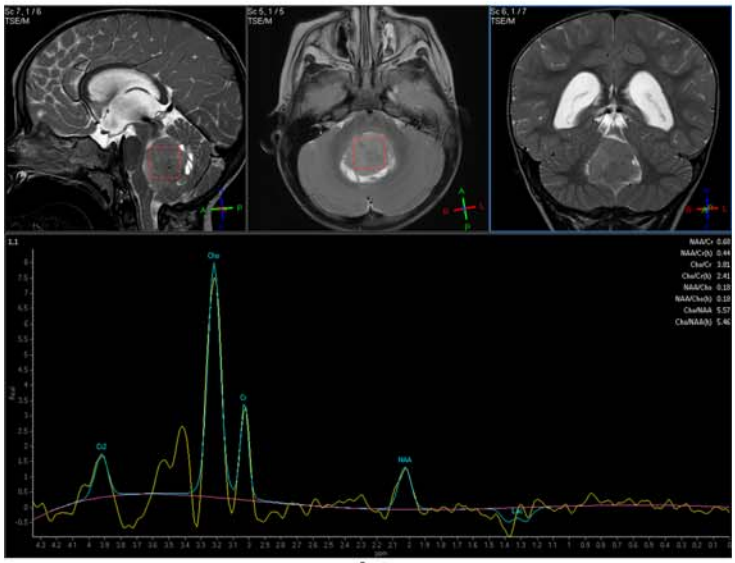

b

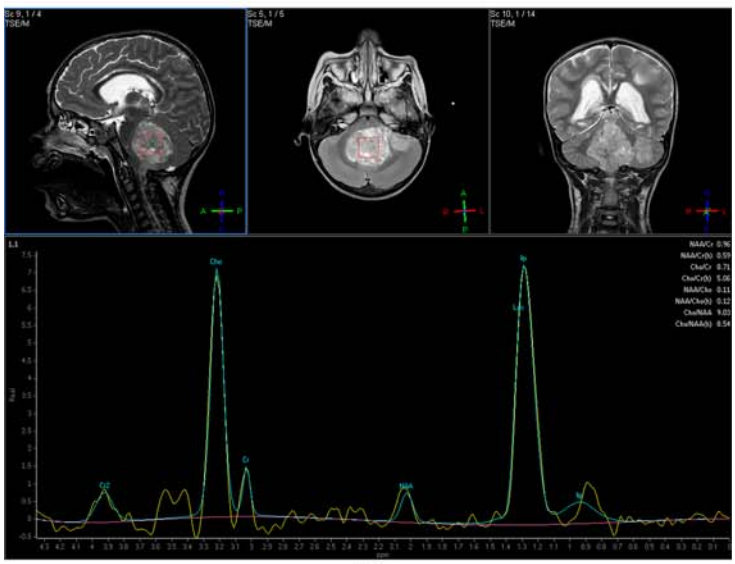

c

Fig. 8 Proton MRS (PRESS, TE 144 ms) in medulloblastomas (grade IV). **a** Anaplastic medulloblastoma of the left cerebellar hemisphere in a 3-year-old boy. There is marked increase of Cho/Cr and profound reduction of NAA/Cr. Although creatine levels are often relatively stable in the brain, creatine consumption due to energy impairment likely contributes to this spectrum. **b** Classic vermian medulloblastoma in a 2-year-old boy. There is increase of Cho/Cr and reduction of NAA/Cr, although perhaps not as extreme as in the previous case. Notice taurine peak at 3.4 ppm. **c** Anaplastic medulloblastoma in a 4-year-old girl. Note very prominent lipid peak, consistent with necrosis in this very aggressive medulloblastoma variant

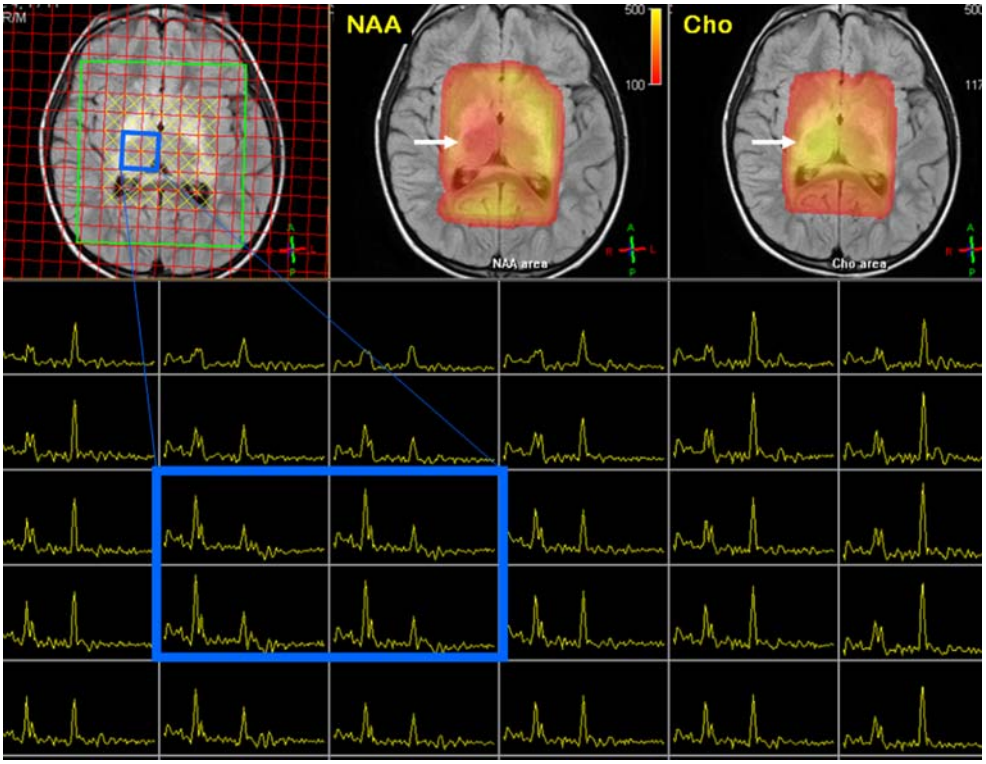

Fig. 9 Chemical shift imaging in a 6-year-old boy with gliomatosis cerebri involving the nucleocapsular regions of both hemispheres. Among available spectra, a region (*blue*) corresponding to the right thalamus shows higher Cho/Cr and lower NAA/Cr than the remaining tumour infiltration. Colour maps (upper right) confirm absolute increase of Cho and decrease of NAA concentrations (*arrows*)

Conclusion

Functional MRI techniques, including MR diffusion (complemented with diffusion tensor imaging/fibre tractography), perfusion and spectroscopy, have contributed significantly to the pre- and postoperative assessment of brain tumours in children. These techniques should be used as complementary tools to conventional MRI as they provide additional information on biological, physiological and metabolic features of brain tumours that are not available based on conventional MRI studies. On the other hand, the implementation of these techniques has significantly increased the duration of MRI examinations, introducing new challenges to work organization and safety issues. Therefore, it is important that the scanning protocol is tailored to the individual case in order to avoid unnecessary scanning while maximizing the amount of information, both anatomic and functional, that is made available to the clinician. The advent of higher field strength magnets is expected to improve the rapidity and yield of these techniques, leading to an increase in their application both to presurgical imaging and treatment response monitoring.

References

1. Poussaint TY, Rodriguez D (2006) Advanced neuroimaging of pediatric brain tumors: MR diffusion, MR perfusion, and MR spectroscopy. Neuroimaging Clin N Am 16:169–192
2. Bükte Y, Paksoy Y, Genç E et al (2005) Role of diffusion-weighted MR in differential diagnosis of intracranial cystic lesions. Clin Radiol 60:375–383
3. Tsuruda JS, Chew WM, Moseley ME et al (1990) Diffusion-weighted MR imaging of the brain: value of differentiating between extraaxial cysts and epidermoid tumors. AJNR 11:925–931
4. Yamasaki F, Kurisu K, Satoh K et al (2005) Apparent diffusion coefficient of human brain tumors at MR imaging. Radiology 235:985–991
5. Jellison BJ, Field AS, Medow J et al (2004) Diffusion tensor imaging of cerebral white matter: a pictorial review of physics, fiber tract anatomy, and tumor imaging patterns. AJNR 25:356–369
6. Covarrubias DJ, Rosen BR, Lev MH (2004) Dynamic magnetic resonance perfusion imaging of brain tumors. Oncologist 9:528–537
7. Lacerda S, Law M (2009) Magnetic resonance perfusion and permeability imaging in brain tumors. Neuroimaging Clin N Am 19:527–557
8. Cha S (2006) Dynamic susceptibility-weighted contrast-enhanced perfusion MR imaging in pediatric patients. Neuroimaging Clin N Am 16:137–147
9. Provenzale JM, Wang GR, Brenner T et al (2002) Comparison of permeability in high-grade and low-grade brain tumors using dynamic susceptibility contrast MR imaging. AJR 178:711–716
10. Lüdemann L, Warmuth C, Plotkin M et al (2009) Brain tumor perfusion: comparison of dynamic contrast enhanced magnetic resonance imaging using T1, T2, and T2* contrast, pulsed arterial spin labeling, and H2(15)O positron emission tomography. Eur J Radiol 70:465–474
11. Law M, Yang S, Wang H et al (2003) Glioma grading: sensitivity, specificity, and predictive values of perfusion MR imaging and proton MR spectroscopic imaging compared with conventional MR imaging. AJNR 24:1989–1998
12. Shin JH, Lee HK, Kwun BD et al (2002) Using relative cerebral blood flow and volume to evaluate the histopathologic grade of cerebral gliomas: preliminary results. AJR 179:783–789

13. Tzika AA, Astrakas LG, Zarifi MK et al (2004) Spectroscopic and perfusion magnetic resonance imaging predictors of progression in pediatric brain tumors. Cancer 100:1246–1256
14. Cha S (2004) Perfusion MR imaging of brain tumors. Top Magn Reson Imaging 15:279–289
15. Barajas RF Jr, Chang JS, Segal MR et al (2009) Differentiation of recurrent glioblastoma multiforme from radiation necrosis after external beam radiation therapy with dynamic susceptibility-weighted contrast-enhanced perfusion MR imaging. Radiology 253:486–496
16. Warren KE (2004) NMR spectroscopy and pediatric brain tumors. Oncologist 9:312–318
17. Astrakas LG, Zurakowski D, Tzika AA et al (2004) Noninvasive magnetic resonance spectroscopic imaging biomarkers to predict the clinical grade of pediatric brain tumors. Clin Cancer Res 10:8220–8228
18. Hwang JH, Egnaczyk GF, Ballard E et al (1998) Proton MR spectroscopic characteristics of pediatric pilocytic astrocytomas. AJNR 19:535–540
19. Cho YD, Choi GH, Lee SP et al (2003) (1)H-MRS metabolic patterns for distinguishing between meningiomas and other brain tumors. Magn Reson Imaging 21:663–672
20. Kovanlikaya A, Panigrahy A, Krieger MD et al (2005) Untreated pediatric primitive neuroectodermal tumor in vivo: quantitation of taurine with MR spectroscopy. Radiology 236:1020–1025